blood®
Regular Article

LYMPHOID NEOPLASIA

Distinct molecular profile of *IRF4*-rearranged large B-cell lymphoma

Joan Enric Ramis-Zaldivar,[1,2,*] Blanca Gonzalez-Farré,[1-3,*] Olga Balagué,[3] Verónica Celis,[4] Ferran Nadeu,[1,2] Julia Salmerón-Villalobos,[1] Mara Andrés,[5] Idoia Martin-Guerrero,[6,7] Marta Garrido-Pontnou,[8] Ayman Gaafar,[9] Mariona Suñol,[10] Carmen Bárcena,[11] Federico Garcia-Bragado,[12] Maitane Andión,[13] Daniel Azorín,[14] Itziar Astigarraga,[7] Maria Sagaseta de Ilurdoz,[15] Constantino Sábado,[16] Soledad Gallego,[16] Jaime Verdú-Amorós,[17] Rafael Fernandez-Delgado,[17] Vanesa Perez,[18] Gustavo Tapia,[19] Anna Mozos,[20] Montserrat Torrent,[21] Palma Solano-Páez,[22] Alfredo Rivas-Delgado,[3] Ivan Dlouhy,[3] Guillem Clot,[1,2] Anna Enjuanes,[1,2] Armando López-Guillermo,[3] Pallavi Galera,[23] Matthew J. Oberley,[24] Alanna Maguire,[25] Colleen Ramsower,[25] Lisa M. Rimsza,[26] Leticia Quintanilla-Martinez,[27] Elaine S. Jaffe,[23] Elías Campo,[1-3] and Itziar Salaverria[1,2]

[1]Institut d'Investigacions Biomèdiques August Pi i Sunyer, Barcelona, Spain; [2]Centro de Investigación Biomédica en Red de Cáncer, Madrid, Spain; [3]Hematopathology Unit, Hospital Clínic de Barcelona, University of Barcelona, Barcelona, Spain; [4]Pediatric Oncology Department, Hospital Sant Joan de Déu, Esplugues de Llobregat, Spain; [5]Pediatric Oncology Department, Hospital Universitario y Politécnico La Fe de Valencia, Valencia, Spain; [6]Department of Genetics, Physical Anthropology, and Animal Physiology, Faculty of Science and Technology, University of the Basque Country, Universidad del Pais Vasco/Euskal Herriko Unibertsitatea, Leioa, Spain; [7]Pediatric Oncology Unit, Hospital Universitario Cruces Osakidetza, Biocruces Bizkaia Health Research Institute, Barakaldo, Spain; [8]Pathology Department, Hospital Universitari Vall d'Hebron, Barcelona, Spain; [9]Pathology Department, Hospital Universitario Cruces Osakidetza, Biocruces Bizkaia Health Research Institute, Barakaldo, Spain; [10]Pathology Department, Hospital Sant Joan de Déu, Esplugues de Llobregat, Spain; [11]Pathology Department, Hospital Universitario 12 de Octubre, Madrid, Spain; [12]Pathology Department, Complejo Hospitalario de Navarra, Pamplona, Spain; [13]Pediatric Oncology Department and [14]Pathology Department, Hospital Universitario Infantil Niño Jesus, Madrid, Spain; [15]Pediatric Oncology Department, Complejo Hospitalario de Navarra, Pamplona, Spain; [16]Pediatric Oncology Department, Hospital Universitari Vall d'Hebron, Barcelona, Spain; [17]Pediatric Oncology Department, Hospital Clínico Universitario de Valencia, Valencia, Spain; [18]Pediatric Oncology Department, Hospital Universitario 12 de Octubre, Madrid, Spain; [19]Pathology Department, Hospital Trias i Pujol, Badalona, Spain; [20]Pathology Department and [21]Pediatric Oncology Department, Hospital de Sant Pau i la Santa Creu, Barcelona, Spain; [22]Pediatric Oncology Department, Hospital Virgen del Rocio, Sevilla, Spain; [23]Laboratory of Pathology, National Institutes of Health, Bethesda, MD; [24]Department of Pathology and Laboratory Medicine, Children's Hospital Los Angeles, Los Angeles, CA; [25]Department of Research, Mayo Clinic, Scottsdale, AZ; [26]Department of Laboratory Medicine and Pathology, Mayo Clinic, Phoenix, AZ; and [27]Institute of Pathology, University Hospital Tübingen, Eberhard Karls University of Tübingen, Tübingen, Germany

KEY POINTS

- **LBCL with *IRF4* rearrangement displays a mutational profile distinct from other LBCLs affecting pediatric and young adult patients.**
- **Age, high genetic complexity, ABC profile, and *TP53* mutations are associated with poor prognosis in pediatric and young adult LBCL.**

Pediatric large B-cell lymphomas (LBCLs) share morphological and phenotypic features with adult types but have better prognosis. The higher frequency of some subtypes such as LBCL with *IRF4* rearrangement (LBCL-*IRF4*) in children suggests that some age-related biological differences may exist. To characterize the genetic and molecular heterogeneity of these tumors, we studied 31 diffuse LBCLs (DLBCLs), not otherwise specified (NOS); 20 LBCL-*IRF4* cases; and 12 cases of high-grade B-cell lymphoma (HGBCL), NOS in patients ≤25 years using an integrated approach, including targeted gene sequencing, copy-number arrays, and gene expression profiling. Each subgroup displayed different molecular profiles. LBCL-*IRF4* had frequent mutations in *IRF4* and NF-κB pathway genes (*CARD11*, *CD79B*, and *MYD88*), losses of 17p13 and gains of chromosome 7, 11q12.3-q25, whereas DLBCL, NOS was predominantly of germinal center B-cell (GCB) subtype and carried gene mutations similar to the adult counterpart (eg, *SOCS1* and *KMT2D*), gains of 2p16/*REL*, and losses of 19p13/*CD70*. A subset of HGBCL, NOS displayed recurrent alterations of Burkitt lymphoma–related genes such as *MYC*, *ID3*, and *DDX3X* and homozygous deletions of 9p21/*CDKN2A*, whereas other cases were genetically closer to GCB DLBCL. Factors related to unfavorable outcome were age >18 years; activated B-cell (ABC) DLBCL profile, HGBCL, NOS, high genetic complexity, 1q21-q44 gains, 2p16/*REL* gains/amplifications, 19p13/*CD70* homozygous deletions, and *TP53* and *MYC* mutations. In conclusion, these findings further unravel the molecular heterogeneity of pediatric and young adult LBCL, improve the classification of this group of tumors, and provide new parameters for risk stratification. (*Blood*. 2020;135(4):274-286)

Introduction

Large B-cell lymphomas (LBCLs) in children and young adults have morphological and phenotypic features similar to those observed in their adult counterparts. However, the more favorable outcome of most pediatric patients after high-dose chemotherapy may be due, among other factors, to a different underlying biology.[1] Recent molecular studies of diffuse LBCLs (DLBCLs) not otherwise specified (NOS) in adults revealed that

the heterogeneity of these tumors is mainly related to cell-of-origin (COO) subtyping into germinal center B cells (GCBs) or activated B cells (ABCs), and a plethora of genomic alterations defining specific clusters with different clinical manifestations and outcome.[2-7]

Aggressive mature B-cell lymphomas in children and young adults include Burkitt lymphoma (BL), primary mediastinal large B-cell lymphoma (PMBL), and DLBCL, NOS. The first 2 subtypes have been extensively studied with now well-established profiles of genomic alterations.[8-12] However, the molecular characterization of DLBCL, NOS in this age group is less defined. In fact, the constellation of LBCL in these patients seems more diverse than initially recognized. Clinicopathologic studies of LBCL in children have identified 2 additional tumors subtypes, included in the recent update of the World Health Organization (WHO) classification as provisional entities, that have overlapping features with BL and DLBCL.[13] Burkitt-like lymphoma with 11q aberration (BLL-11q) is a high-grade B-cell lymphoma (HGBCL) that was initially considered BL related but without *MYC* translocations.[14] However, 2 recent molecular studies have identified that these tumors lack the common BL mutations in the TCF3-ID3 axis and carry alterations closer to those found in GCB-DLBCL, although with differences suggesting they are a specific DLBCL subtype.[15,16] LBCL with *IRF4* rearrangement (LBCL-*IRF4*) predominates in pediatric population, has a favorable outcome after therapy, and consistently expresses IRF4 due to translocation.[17-20] These cases display a complex pattern of chromosomal changes, but their mutational profile and possible relationship to other LBCLs is not known.[21] The last WHO classification has also recognized the category of HGBCL that encompasses a spectrum of morphological appearances from blastoid to cases with intermediate features between BL and DLBCL.[13] The mutational profile of these tumors is not well known, but some studies in adults have identified the simultaneous presence of characteristic mutations of both BL and DLBCL.[22,23] The genomic features of these tumors in pediatric populations and their relationship to other LBCLs in this group of patients are not known.

Pediatric LBCLs and BL are treated using the same therapeutic protocols.[1,24] Although generally curable with this intensive chemotherapy, ~10% of cases relapse.[1] Biological prognostic parameters predicting an adverse outcome have been extensively studied in adult DLBCL[5,6,25,26] but are less well defined in pediatric and young adult tumors, with only few studies reported.[24,27] A better understanding of the molecular pathogenesis of these tumors may assist in defining management protocols better suited to the biology of the disease. In the present study, we aimed to extensively characterize the molecular landscape of LBCL in the pediatric and young adult population and identify clinically relevant molecular features specific to different subtypes that are distinct from adult cases.

Methods

Patients and samples

Sixty-three patients <26 years with LBCL were included in the study and centrally reviewed by 3 hematopathologists (B.G.-F., O.B., and E.C.). Cases were classified according to WHO criteria[13] into DLBCL, NOS (n = 31); LBCL-*IRF4* (n = 20); and HGBCL, NOS (n = 12). No HGBCLs with *MYC* and *BCL2*/*BCL6* rearrangements were identified. Fifty-three cases (51 primary and 2 relapses obtained 10 and 23 months after first diagnosis) were gathered in a centralized review supported by Sociedad Española de Hematología y Oncología Pediátrica or from the hematopathology files of Hospital Clínic of Barcelona, Spain. Additionally, 9 LBCL-*IRF4* and 1 DLBCL, NOS were consultation cases from the University of Tübingen (Tübingen, Germany), National Institutes of Health (Bethesda, MD), and Children's Hospital Los Angeles (Los Angeles, CA). Moreover, samples at relapse from 3 patients with primary tumor available were investigated. BL, BLL-11q, and PMBL cases were excluded. This study was approved by our institutional review board and in accordance with the Declaration of Helsinki.

Immunohistochemistry and FISH

Immunohistochemistry and fluorescence in situ hybridization (FISH) analyses were performed using standard protocols. The morphology, growth pattern, cytology, and immunohistochemical stains together with Epstein-Barr virus (EBV) in situ hybridization were evaluated as part of the diagnostic workup (supplemental Table 1, available on the *Blood* Web site). Cases were classified as germinal center (GC) and non-GC subtypes according to the Hans algorithm.[28] Genetic alterations of *BCL2*, *BCL6*, *MYC*, *IRF4*, *CIITA*, and IGH were analyzed by commercial (Metasystems, Altlußheim, Germany) or homemade FISH probes.[17,29]

Targeted NGS and mutational analysis

Fifty-five LBCLs from 52 patients were examined for the mutational status of 96 B-cell lymphoma–related genes (supplemental Table 2) using the SureSelectXT Target Enrichment System Capture next-generation sequencing (NGS) strategy library (Agilent Technologies, Santa Clara, CA) before sequencing on MiSeq equipment (Illumina, San Diego, CA) (supplemental Methods; supplemental Figures 1 and 2). The contribution of previously defined mutational signatures was calculated for each gene (supplemental Methods). Variant verification was performed using the Ampliseq NGS method (Illumina) (supplemental Table 3) and/or by Sanger sequencing analysis using the primers detailed in supplemental Table 4. The previously published mutational profile of 144 adult DLBCLs was used for comparisons.[26]

DNA CN alteration analysis

Copy-number (CN) alterations were examined in 59 LBCLs from 55 patients using Oncoscan or single-nucleotide polymorphism array platforms (Thermo Fisher Scientific, Waltham, MA) according to standard protocols (supplemental Methods). Gains and losses and CN neutral loss of heterozygosity (CNN-LOH) regions were evaluated using Nexus Biodiscovery v9.0 software (Biodiscovery, Hawthorne, CA). Additional previously published CN data were used for comparison.[26,30]

Gene expression profile by NanoString

COO classification was performed using Lymph2Cx assay (NanoString, Seattle, WA).[31] The Lymph3Cx assay was used for detection of molecular PMBL (mPMBL).[32] The NanoString Pan-Cancer Immune Profiling Panel was also used to investigate additional gene expression differences between different subsets of LBCL (supplemental Methods).

Statistical methods

Survival probabilities were estimated with the Kaplan-Meier method and differences assessed by the log-rank test. Event-free survival (EFS) was calculated as previously described.[33] Differences in the distribution of individual parameters among patient subsets were analyzed by Fisher's exact test for categorized variables, and the Student *t* test for continuous variables. Nonparametric tests were applied when necessary. Only mutations and genomic aberrations present in 5% of the cases and affecting a minimum of 4 cases were accounted for comparisons. The *P* values for multiple comparisons were adjusted using the Benjamini-Hochberg correction (false discovery rate). A cutoff of $P = .05$ was considered significant unless otherwise indicated. Statistical analyses were carried out using R software v3.5.0.

Results

Clinicopathological characteristics

Twenty cases were classified as LBCL-*IRF4* (11 females, 9 males; median age, 14 years; range, 5-22 years). Eight patients had nodal involvement, mainly in the head and neck region, and 8 had tonsillar disease (Table 1). The other 4 patients (20%) had primary extranodal presentation in the gastrointestinal tract (2 cases), liver, and larynx. Histologically, 9 cases were purely diffuse, 5 cases showed a nodular growth pattern, and 6 displayed both follicular and diffuse areas. All cases showed positivity for MUM1/IRF4 and BCL6, whereas CD10 and BCL2 were positive in 11 and 10 cases, respectively (Figure 1). Five out of 12 cases coexpressed CD5, and all cases analyzed were negative for EBV. FISH studies identified the *IRF4* translocation in 17 out of the 19 investigated cases, and the remaining 2 negative cases had breaks of the IGH locus (Figure 2). None of the 11 LBCL-*IRF4* cases interrogated carried *BCL6* or *BCL2* rearrangements. The Lymph2Cx assay predicted 10 cases (72%) as GCB, 3 (21%) as unclassified, and only 1 (7%) as ABC. The IRF4/MUM1 messenger RNA levels detected by this assay were significantly higher than in DLBCL, NOS and HGBCL, NOS ($P < .01$) (supplemental Figure 3).

Thirty-one cases (22 males and 9 females; median age, 14 years; range, 1-25 years) were classified as DLBCL, NOS, all with a diffuse pattern of large, mainly centroblastic cells. Most cases showed a GC-phenotype (20/31, 65%) in line with the Lymph2Cx results that showed a GCB profile in 67%, followed by 22% ABC and 11% UNC. *MYC* breaks were detected in 3 cases, *BCL6* rearrangement in 2 cases (supplemental Table 5), and, contrary to adult DLBCL, NOS, only 1 case presented *BCL2* translocation. EBV was positive in 5 out of 25 (20%) cases, 4 of which had an ABC phenotype. Seven patients had primary extranodal presentation.

Finally, 12 cases were classified as HGBCL, NOS (8 males and 4 females; median age, 9.5 years; range, 3-23 years), 8 with intermediate features between DLBCL and BL and 4 with blastoid morphology (Figure 3). These cases mainly had a GC phenotype (91%) and were classified as GCB (7/9 cases) by the Lymph2Cx assay. Inmunohistochemically, BCL2 was positive in 5 out of 11 cases (45%) and MYC in 3, but without typical BL morphology (supplemental Figure 4). *MYC* and *BCL6* translocations were detected in 4 cases and 1 case, respectively. No double/triple hits were identified. EBV was detected in 2 cases. Most patients had a primary extranodal presentation (75%) (Figure 2; supplemental Table 6).

A recent gene expression study has recognized PMBL at non-mediastinal sites and/or with atypical clinical presentations.[34] To identify any potential PMBL not recognized based on conventional clinicopathological criteria, we investigated the mPMBL signature using the Lymph3Cx assay[32] in 39 cases (21 DLBCL, NOS; 14 LBCL-IRF4; and 4 HGBCL, NOS) with available RNA. This analysis predicted 4 DLBCL, NOS as mPMBL. Three of these cases had mediastinal involvement but were not considered initially as PMBL due to concomitant disseminated disease involving bone marrow, lymph nodes, and multiple extranodal sites (supplemental Table 7). However, 1 DLBCL, NOS case predicted as mPMBL had a solitary axillary lymph node without apparent mediastinal involvement. These 4 cases were analyzed as a separate category in subsequent molecular analyses. Finally, the assay predicted 5 DLBCL, NOS, as "uncertain," ie, with a gene expression signature probability score between DLBCL and PMBL. None of these 5 cases had clinicopathological features of PMBL (supplemental Table 7). Additionally, Lymph2Cx/Lymph3Cx had 100% concordance for COO prediction (Figure 2).

Identification of mutational profiles by targeted NGS

Fifty-five tumors (50 primary, including 22 DLBCL, NOS; 17 LBCL-*IRF4*; 8 HGBCL, NOS; 3 mPMBL; and 5 relapsed samples) were analyzed by NGS (mean coverage, 447×; range, 28-1439×). After filtering, 496 mutations were identified in 50 out of 55 samples analyzed with a verification rate of 97% (147/151) of the selected variants (supplemental Table 8). A total of 331 variants (67%) were predicted as potential driver mutations (supplemental Methods). After exclusion of mPMBL and relapsed samples, the remaining 47 cases displayed a total of 245 driver mutations with a mean of 5.2 driver mutations per case. The most recurrently mutated genes were *IRF4* (14/47, 30%), *CARD11* and *CCND3* (8/47, 17%), *KMT2D*, *MYC*, *PIM1*, or *SOCS1* (6/47, 13%), and *FOXO1* (5/47, 11%) (Figure 4A).

The number of mutations per case was similar among the 3 subtypes (mean: LBCL-*IRF4*, 5.2 mutations/case; DLBCL, NOS, 5.8; and HGBCL, NOS, 6.6), but they exhibited different mutational profiles (Figure 4). The most frequently mutated genes in LBCL-*IRF4* were *IRF4* (76%), *CARD11* (35%), and *CCND3* (24%). Interestingly, mutations in 3 genes activating the NF-κB pathway (*CARD11*, *CD79B*, and *MYD88*) were observed in 6 out of the 17 analyzed cases. Of note, these 6 cases showed a purely diffuse morphology. The majority of *CARD11* mutations (4/6) occurred in the coiled-coil domain, which is known to produce a constitutive NF-κB activation and enhanced NF-κB activity in adult DLBCL.[35] All *CD79B* mutated cases carried a Y197 hot spot mutation affecting the immunoreceptor tyrosine-based activation motif domain (Figure 4B). Mutations on this residue reduce its negative regulation by the kinase LYN.[36] *MAP2K1* mutations, typically seen in pediatric-type follicular lymphoma, were detected in 2 cases with predominant follicular growth pattern and confirmed *IRF4*-rearrangement (supplemental Figure 5).[37,38] Multiple *IRF4* mutations (>4 mutations/case including synonymous variants) were observed in 9 cases, all of which carried the *IRF4* rearrangement. These mutations had the pattern of aberrant somatic hypermutation (aSHM) and predominant AID

Table 1. Pathological and clinical features of 20 LBCL cases with *IRF4* rearrangement

Case	Age (y), gender	Biopsy site	Growth pattern	Immunohistochemistry				FISH		COO NanoString (Lymph2Cx)	Stage*	Treatment	Outcome, follow-up
				CD10	BCL6	BCL2	IRF4/MUM1	*IRF4*	IGH				
D1	5, F	LN	Follicular and diffuse	+	+	+	+						
D2	14, M	LN	Follicular	+	+	−	+	R		GCB		Surgical excision	
D15	5, F	Tonsil	Diffuse	−	+	+	+	R	R	GCB	II	CT-P	CR, 49 mo
D16	14, F	Tonsil	Diffuse	−	+	−	+	R			II	CT-P	CR, 99 mo
D17	21, M	Liver	Diffuse	−	+	+	+	R		ABC	I-E	CT-A	CR, 10 mo †
D20	17, M	Ileum	Diffuse	+	+	+	+	N	R	UNC	II	CT-P	CR, 72 mo
D21	8, M	Tonsil	Follicular	+	+	+	+	R			I	CT-P	CR, 36 mo
D23	21, F	Inguinal LN	Diffuse	−	+		+	R	R	GCB	IV-A	CT-A	CR, 40 mo
D31	12, F	Cervical LN	Diffuse	−	+	+	+	N	R	UNC			
D32	7, M	Tonsil	Follicular	+	+	+	+	R		GCB	I	CT-P	CR, 22 mo
D35	6, F	Cervical LN	Diffuse	+	+	−	+	R		GCB	I	CT-P	CR, 63 mo
D46	11, M	Tonsil	Follicular and diffuse	+	+	−	+	R	R	GCB		Surgical excision	
D47	22, M	Tonsil	Follicular and diffuse	+	+	−	+	R	R		I	CT-A	CR, 24 mo
D48	18, F	Tonsil	Follicular and diffuse	−	+	−	+	R		UNC	I	CT-A	CR, 29 mo
D50	17, F	Cervical LN	Follicular	−	+	−	+	R	R			Surgical excision	
D51	10, F	Tonsil	Follicular and diffuse	+	+	−	+	R		GCB	III	CT-P	CR, 14 mo
D54	18, F	Cervical LN	Diffuse	+	+	+	+	R		GCB	III	CT-P	CR, 14 mo
D62	17, M	Cervical LN	Follicular	−	+	−	+	R		GCB	II	CT-P	CR, 45 mo
D63	14, F	Larynx	Diffuse	+	+	+	+	R		GCB	I	CT-P	CR, 18 mo
D69	15, M	Intestine	Follicular and diffuse	−	+	+	+	R				CT-P	CR, 10 mo

CR, complete response; CT-A, chemotherapy with adult schema protocol (R-CHOP/ESHAP); CT-P, chemotherapy with pediatric schema protocol; F, female; LN, lymph node; M, male; N, normal; R, rearrangement; UNC, intermediate/unclassified.

*Stage was established according St. Jude/International Pediatric NHL Staging System or Ann Arbor staging system for pediatric and adult patients, respectively.

†Patients who had a relapse/progression and needed rescue treatment.

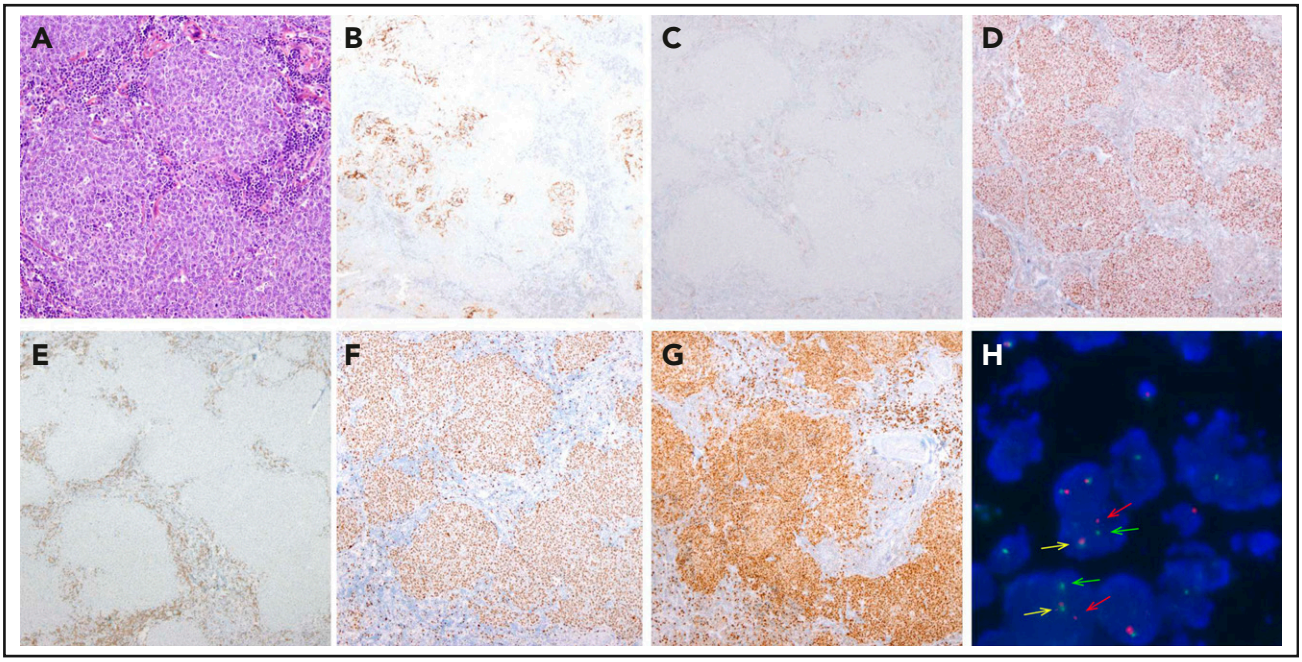

Figure 1. Morphological, immunophenotypic, and genetic features of a LBCL with *IRF4* rearrangement (case D62). Architecture effacement by an atypical lymphoid proliferation with nodular growth pattern (A; hematoxylin and eosin) that corresponds to expanded follicles with highly disrupted follicular dendritic cell meshwork (B; CD21). The atypical cells were negative for CD10 (C) and positive for BCL6 (D). BCL2 was positive in the accompanying reactive T cells but negative in the tumor (E), which exhibits a high proliferation rate (F; Ki67). The immunohistochemical study for IRF4/MUM1 (G; MUM1) shows strong and diffuse positivity in the neoplastic proliferation, and FISH with *IRF4* break-apart probe shows a signal constellation of 1 colocalization (yellow arrow) and 1 split signal (red and green arrows) consistent with the gene rearrangement (H). Original magnification ×100 (A), ×40 (B-G).

mutational signature (supplemental Results; supplemental Figure 6; supplemental Table 9). In agreement with previous observations,[17] 8 out of 16 primary *LBCL-IRF4* cases investigated carried somatic intronic *BCL6* mutations. Of note, these mutations affected the predicted *IRF4*-binding site in 5 cases (supplemental Table 10).[39]

Among the 22 DLBCL, NOS cases, the most frequently mutated genes were *SOCS1* (27%), *KMT2D* (23%), and *BTG1*, *EZH2*, *GNA13*, *MYD88*, and *PIM1* (14%), consistent with a predominantly GCB-DLBCL profile but with absence of *TNFRSF14* and *SGK1* mutations (supplemental Figure 7). Compared with adult DLBCL, NOS, no significant differences were detected in the number of mutations affecting commonly interrogated genes (pediatric/young adult LBCL mean 4.3 vs adult DLBCL 4.8 mutations/case, $P < .15$). However, we observed a higher frequency of *SOCS1* mutations in pediatric and young adult DLBCL, NOS (27% vs 8% respectively, $P = .01$), and the practical absence of some mutations affecting genes was strongly associated with the definition of established mutational clusters in adult DLBCL, NOS, such as *MYD88*-L265P, *NOTCH1*, *NOTCH2*, *BCL2*, and *SGK1* (supplemental Figure 8A).[5,6]

Of the 8 HGBCL, NOS cases examined, 4 had mutations in ≥3 genes predominately associated with BL (supplemental Figure 5). The remaining 4 cases had mutations in *CARD11* (2 cases) or *EZH2* and *TNFRSF14* (1 case each) akin to DLBCL, NOS.[22,23] Interestingly, *MYC* mutations clustered around known phosphorylation sites required for the ubiquitination and degradation of MYC protein as previously described (Figure 4B).[40] Of note, all *MYC* mutated cases (5 HGBCL, NOS and 1 DLBCL, NOS) had multiple mutations (>4 mutations/case including intronic and synonymous variants) with an aSHM pattern (supplemental Table 9).[40,41] Four out of these 6 cases also carried *MYC* rearrangement, and in the 2 remaining ones, the presence of cryptic translocations could not be completely ruled out.[13,42]

We evaluated the presence of recurrent mutated pathways in the different morphological subtypes.[26] This analysis showed frequent mutations in chromatin modifiers in HGBCL, NOS, whereas mutations in B-cell differentiation and JAK-STAT pathway genes were more frequently seen in LBCL-*IRF4* and DLBCL, respectively (supplemental Figure 9).

The mutational profile of the 3 cases predicted as mPMBL was closer to PMBL than DLBCL, NOS, with mutations in *SOCS1*, *NFKBIE*, *STAT6*, *B2M*, and *CIITA*, which appeared to confirm the mPMBL gene expression prediction (supplemental Figure 7).

Finally, the mutational profile of the 3 paired diagnostic-relapse samples analyzed showed marked differences between both biopsy specimens with a total of 13 (mean 4.3, range 0-9) shared and 23 acquired variants (mean 7.7, range 2-16) in the relapsed samples. Additionally, in the 5 relapsed samples available, we identified recurrent *KLHL6* and *BTG2* mutations (2 cases each) (supplemental Figure 10A).

CN alteration profile

CN analysis detected 302 genetic alterations in 43 out of 49 LBCL primary tumors (mean, 6.2 alterations per case; range, 0-34 alterations) and 45 CNN-LOH in 25 out of 49 cases (supplemental Table 11). Recurrent CN alterations (>15%) included gains of 1q21.2-q42.13, 11q22.3-q25, trisomies 7 and 12, and recurrent losses of 1p36.33-p36.13/*TNFRSF14* and 6q21/*PRDM1*.

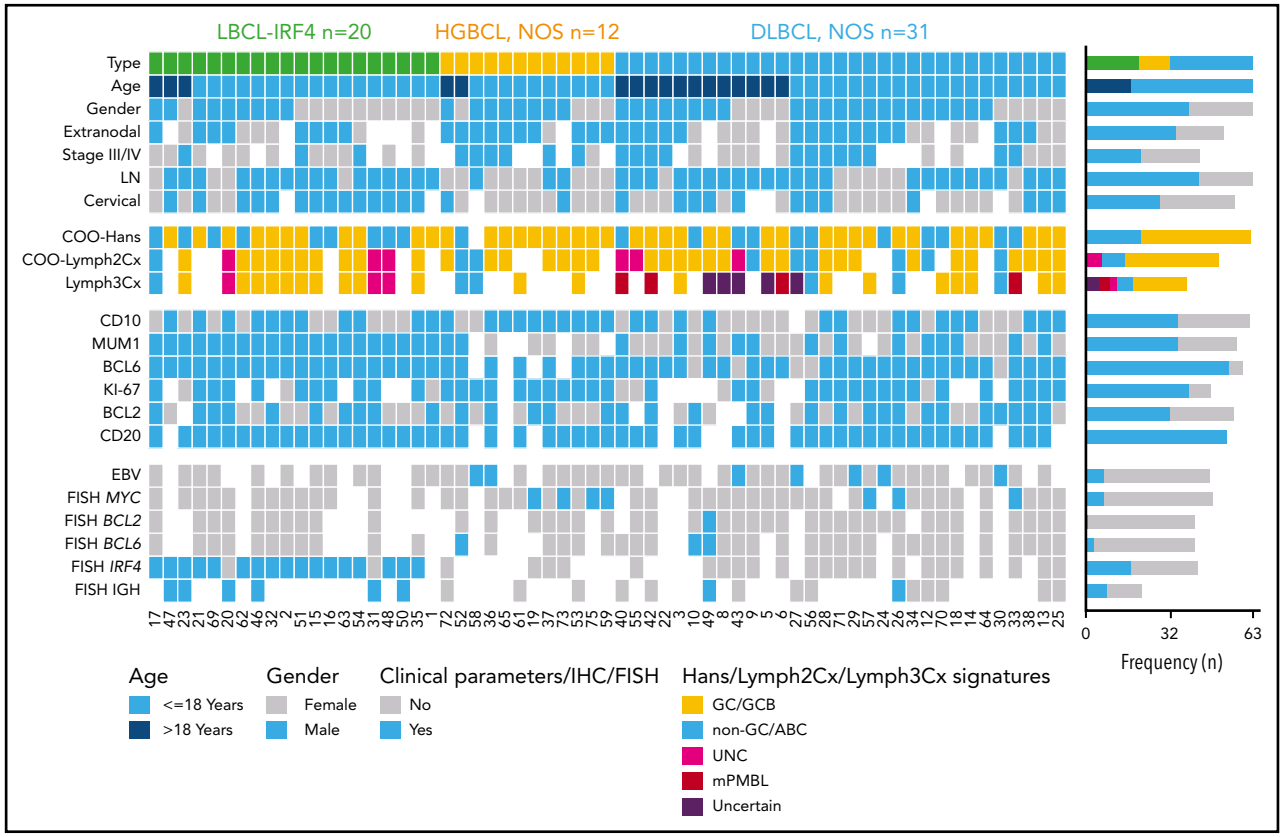

Figure 2. Overview of clinical and histological findings in 63 pediatric and young adult LBCL cases. Each column of the heatmap represents 1 LBCL case and each line a specific analysis. On the right side of the figure, the frequency of the particular result of the analysis is shown. LN, lymph node; UNC, unclassified.

Frequent CNN-LOH (>10%) affected 17q21.3-q25.3 and 19p13.3-p13.2 regions (supplemental Figure 11). Recurrent homozygous deletions were observed at 19p13.3/*CD70* (5 cases) and 9p21.3/*CDKN2A* (3 cases) in addition to single events in 13q14.2/*RB1* and 17q24.1/*GNA13* loci. Alteration patterns suggestive of chromothripsis[43] were found in 4 out of 49 cases (8%) affecting chromosomes 1, 9, 12, and 13, respectively. Of note, all 4 cases carried *MYC, IRF4*, or *BCL6* translocations.

The 3 LBCL subtypes displayed different CN profiles despite having similar number of aberrations (mean, LBCL-*IRF4*, 6.2; DLBCL, NOS, 5.8; and HGBCL, NOS, 7.1 alterations per case). LBCL-*IRF4* had frequent 17p/*TP53* deletions (25%), without gene mutations, and gains of chromosome 7 (45%) and 11q12.3-q25 (35%). DLBCL, NOS had recurrent 2p16 gains targeting *REL* and 19p13 homozygous deletions targeting *CD70* (23% each). HGBCL, NOS had 1q gains (3 cases), similar to BL,[30] but also carried trisomies/gains of 7 (4 cases) and 12 (3 cases), and 9p21.3/*CDKN2A* homozygous deletions (2 cases) (Figure 5).

Compared with adult DLBCL, NOS, pediatric and young adult DLBCL, NOS had a similar CN profile without any specific alteration but significantly lower levels of genetic complexity (mean, 5.8 vs 20 CN alterations; $P < .01$) (supplemental Figure 8B). Our current pediatric and young adult series lacked alterations present in adults such as 6q13-q14.1/*TMEM30A* and 6q22.1-q25.3/*TNFAIP3* deletions as well as those typically associated with ABC-DLBCL as 9p21.3/*CDKN2A* and 17p13.3-p11.2/*TP53* losses, which probably reflects the predominance of GCB cases in our cohort. In fact, these differences were not observed when compared only to adult *BCL2*-negative GCB-DLBCL. Nevertheless, results should be taken with caution, since different CN platforms were used.

Finally, analysis of 3 paired diagnostic-relapsed biopsy specimens showed the acquisition of a mean of 15 additional events (range, 12-16) in the relapsed samples. Recurrent alterations in these cases included gains of 1q21.2-q41 (*MDM4*), 12p13.3-q21.1, and 18q22.2-q23 and biallelic inactivation of 19p13/*CD70*, which was also present in both samples (diagnosis/relapse) in the 3 cases (supplemental Figure 10B) and even in a second relapse in 1 case.

Gene expression patterns

Differential gene expression analysis between LBCL-*IRF4* (n = 11) and DLBCL, NOS (n = 10) identified 48 differentially expressed genes (log2 fold change greater than ±1 and false discovery rate <.05), including 14 NF-κB target genes (29%; eg, *IRF4*, *LTF*, and *CSF1*), which suggests a deregulation of this pathway in LBCL-*IRF4* (http://www.bu.edu/nf-kb/gene-resources/target-genes/) (supplemental Figure 12; supplemental Table 12). No gene expression differences were observed between LBCL-*IRF4* cases with and without *CD79B* or *CARD11* mutations.

Prognostic value of clinical and molecular features

The 5-year EFS of the 46 LBCL patients with available follow-up was 68.4%. All received chemotherapy as first-line treatment, including rituximab in 35% of the patients with no differences in

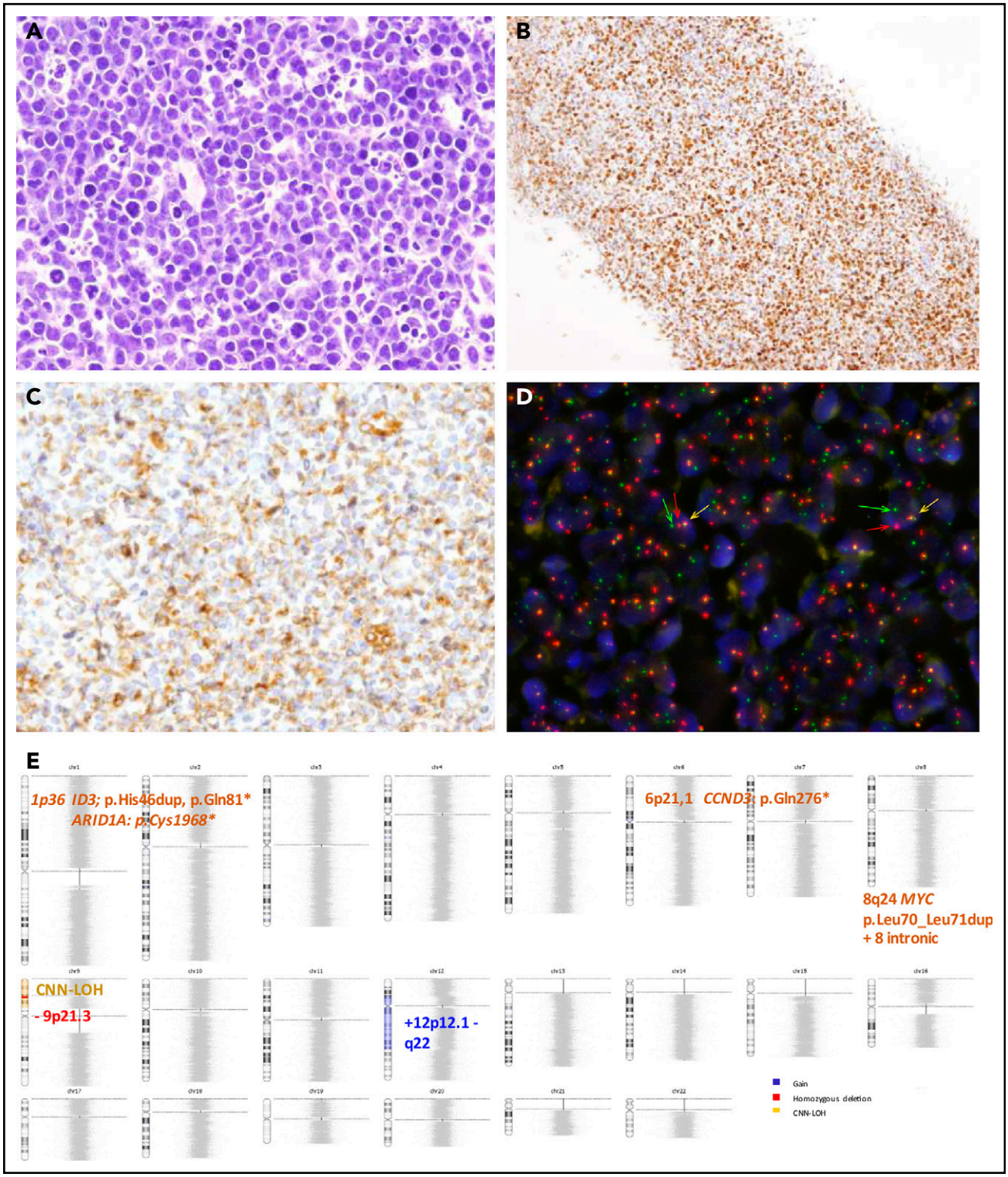

Figure 3. Morphological, immunophenotypic and genetic features of an HGBCL, NOS with *MYC* rearrangement (Case D59). Hematoxylin and eosin stain (A) depicting mild heterogeneity with certain cellular irregularity of the neoplastic cells that are BCL6 positive (B) with partial expression of BCL2 (C). (D) FISH with *MYC* break-apart shows a signal constellation of 1 colocalization (yellow arrow) and 1 split signal (green and red arrows). (E) Ideogram of the CN, CNN-LOH, and mutational features of this case. Original magnification ×400 (A,C), ×100 (B).

EFS (log-rank test $P = .75$). Complete response was achieved in 83% of patients, whereas 8 died of disease. Cases predicted as ABC-DLBCL had significantly worse 5-year EFS compared with GCB-DLBCL patients (26% vs 74% $P = .002$) (Figure 6; supplemental Figure 13), even when the LBCL-*IRF4* cases were excluded from the comparison (30% vs 68%, $P = .033$). Interestingly, the clinical outcome of GCB-DLBCL was similar to LBCL-*IRF4*, whereas ABC-DLBCL and HGBCL, NOS had significantly worse 5-year EFS (78% vs 48%; $P = .005$). Similarly, high lactate dehydrogenase (LDH) levels; a high number of CN

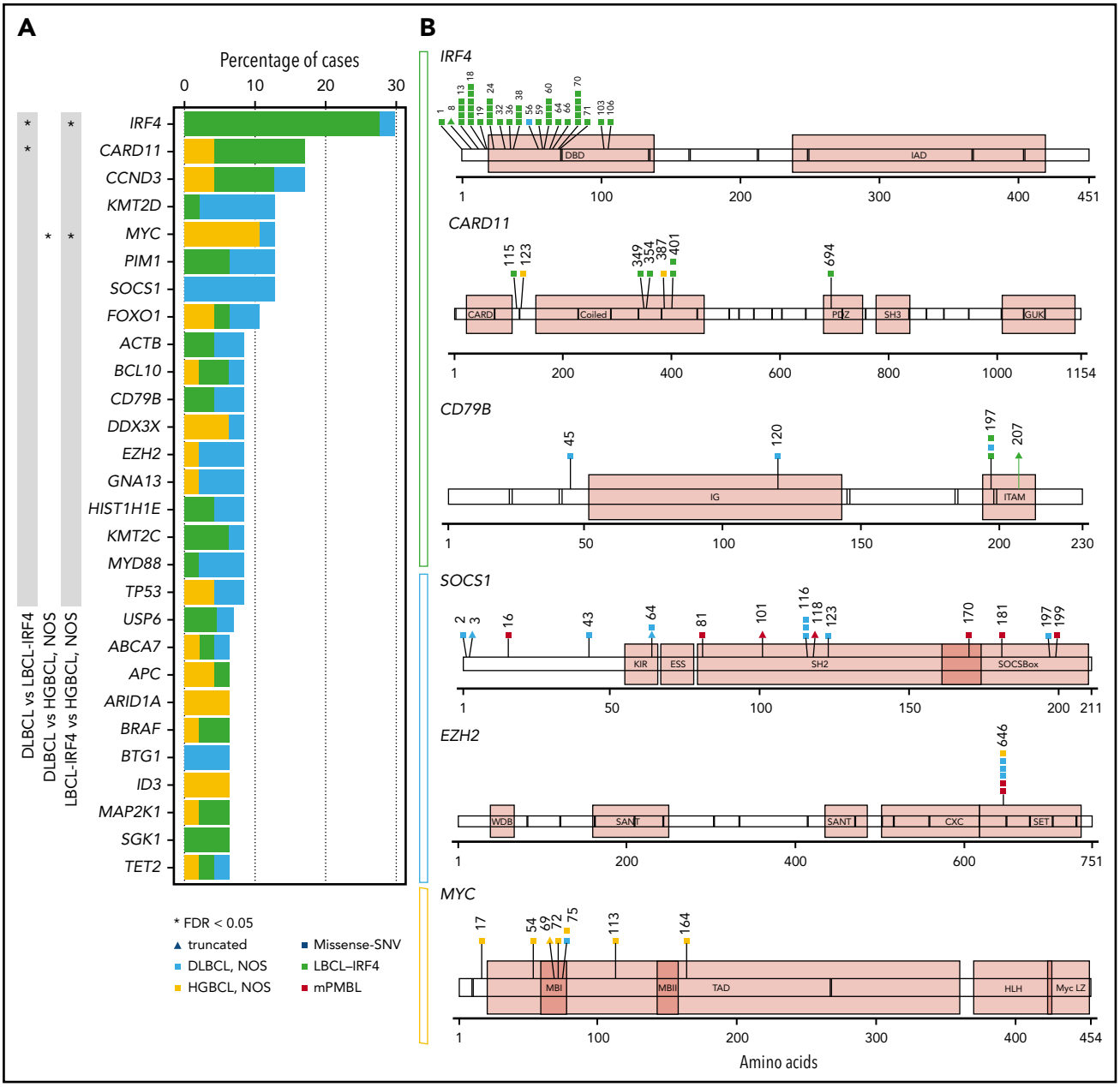

Figure 4. Mutational landscape of 47 pediatric and young adult LBCL cases. (A) Bar graphs show mutated genes in >5% of 47 pediatric and young adult primary LBCL cases excluding mPMBL. Each color bar indicates histological subtypes. An asterisk represents mutated genes significantly enriched in 1 of the subtypes. SNV, single-nucleotide variant. (B) A diagram of the relative positions of driver mutations is shown for *IRF4*, *CARD11*, *CD79B*, *SOCS1*, *EZH2*, and *MYC* genes. x-axes indicate amino acid position: IRF4 domains (DBD, DNA-binding domain; IAD, IRF association domain), CARD11 domains (CARD, caspase activation and recruitment domain; SH, Src homology 3 domain), CD79B domains (IG, immunoglobulin-like; ITAM, immunoreceptor tyrosine-based activation motif), SOCS1 domains (ESS, extended SH2 subdomain; KIR, kinase inhibitory region), EZH2 domains (CXC, cysteine-rich domain; SANT, SWI3-ADA2-*N*-CoR-TFIIIB domains; WDB, WD-40 binding domain), and MYC domains (HLH, helix-loop-helix; LZ, leucine zipper; MBI/II, Myc box I and II; TAD, transactivation domain).

alterations (>10), including cases with chromothripsis-like patterns; *TP53* and *MYC* mutations; gains of 2p16/*REL* and 1q21-q44/*MDM4*; and biallelic inactivation of 19p13/*CD70* correlated with a significant lower EFS rate (Figure 6; supplemental Figure 13).

When patients were examined according to age, pediatric patients (≤18 years) had better 5-year EFS than young adults (19-25 years) (76% vs 46%, log-rank test $P = .044$) (Figure 6; supplemental Figure 13). Young adults had more frequent *BCL6* rearrangements, high genetic complexity, and chromothripsis-like patterns (supplemental Table 13). Finally, when the clinical parameters were compared among the 3 different lymphoma entities, HGBCL, NOS presented more frequently in primary extranodal sites and had a higher incidence of *MYC* rearrangements (supplemental Table 14).

Discussion

Genomic studies of adult LBCL have revealed a large number of somatic mutations and structural alterations related to the

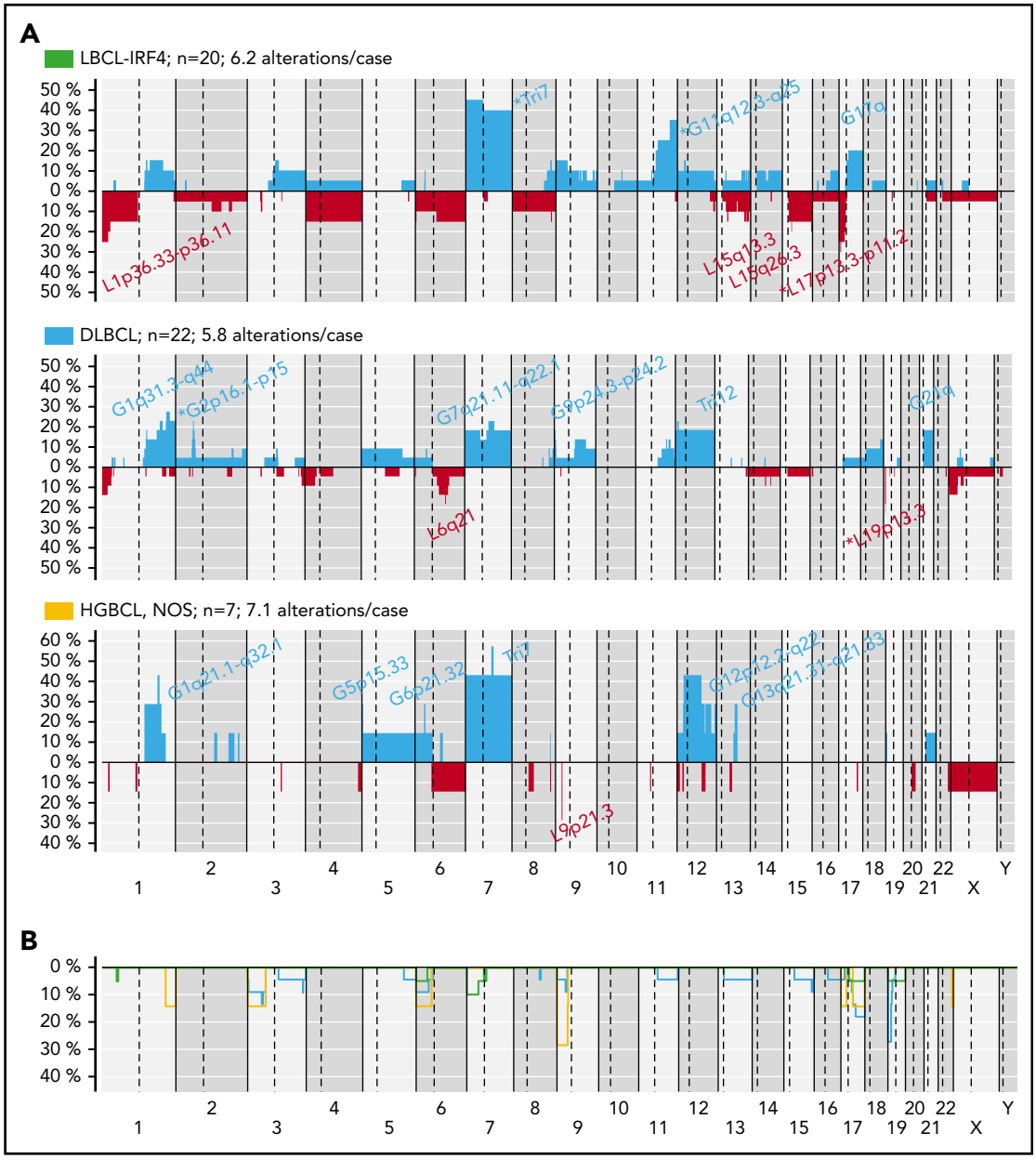

Figure 5. CN profile of pediatric and young adult LBCL cases. (A) Global CN profiles of 20 LBCL-*IRF4* cases; 22 DLBCL, NOS cases; and 7 HGBCL, NOS cases. x-axis indicates chromosomes from 1 to Y and p to q. The vertical axis indicates frequency of each genomic aberration among the analyzed cases. Gains are depicted in blue and losses in red. Most frequently recurrent regions are indicated for LBCL-*IRF4*; DLBCL, NOS (>20%); and HGBCL, NOS (≥2 cases). Asterisks indicate significant differences between LBCL-*IRF4* and DLBCL (Fisher's test, $P < .05$). (B) Comparative plot of CNN-LOH among the 3 morphological groups described above. Green identifies LBCL-*IRF4*; blue DLBCL, NOS; and yellow HGBCL, NOS.

pathogenesis of these diseases.[3,4,7] However, the genetic landscape of these tumors in pediatric populations is poorly known. In this study, through an integrative targeted NGS, CN, and transcriptome data analyses, we show that pediatric and young adult LBCLs are a heterogeneous group of tumors including different entities with specific molecular profiles and clinical behavior. A better understanding of these differences is relevant to design management strategies more adapted to the particular biological behavior of these tumors.

LBCL-*IRF4* was recently recognized as a specific entity genetically characterized b *IRF4* translocation, clinical presentation localized in the head and neck or abdominal regions, and a favorable outcome after chemotherapy.[17,19] We have now expanded these observations to show that these tumors have a distinct molecular profile characterized by frequent mutations in *IRF4* and NF-κB-related genes (*CARD11*, *CD79B*, and *MYD88*) and overexpression of downstream target genes of the NF-κB pathway. These findings are intriguing, because most of these tumors have a GC phenotype and gene expression profile, whereas mutations in these genes and NF-κB activation have mainly been found in ABC-DLBCL in adults.[5] The activation of the NF-κB pathway in these tumors may be also related to the IRF4 overexpression.[44] The presence of multiple mutations

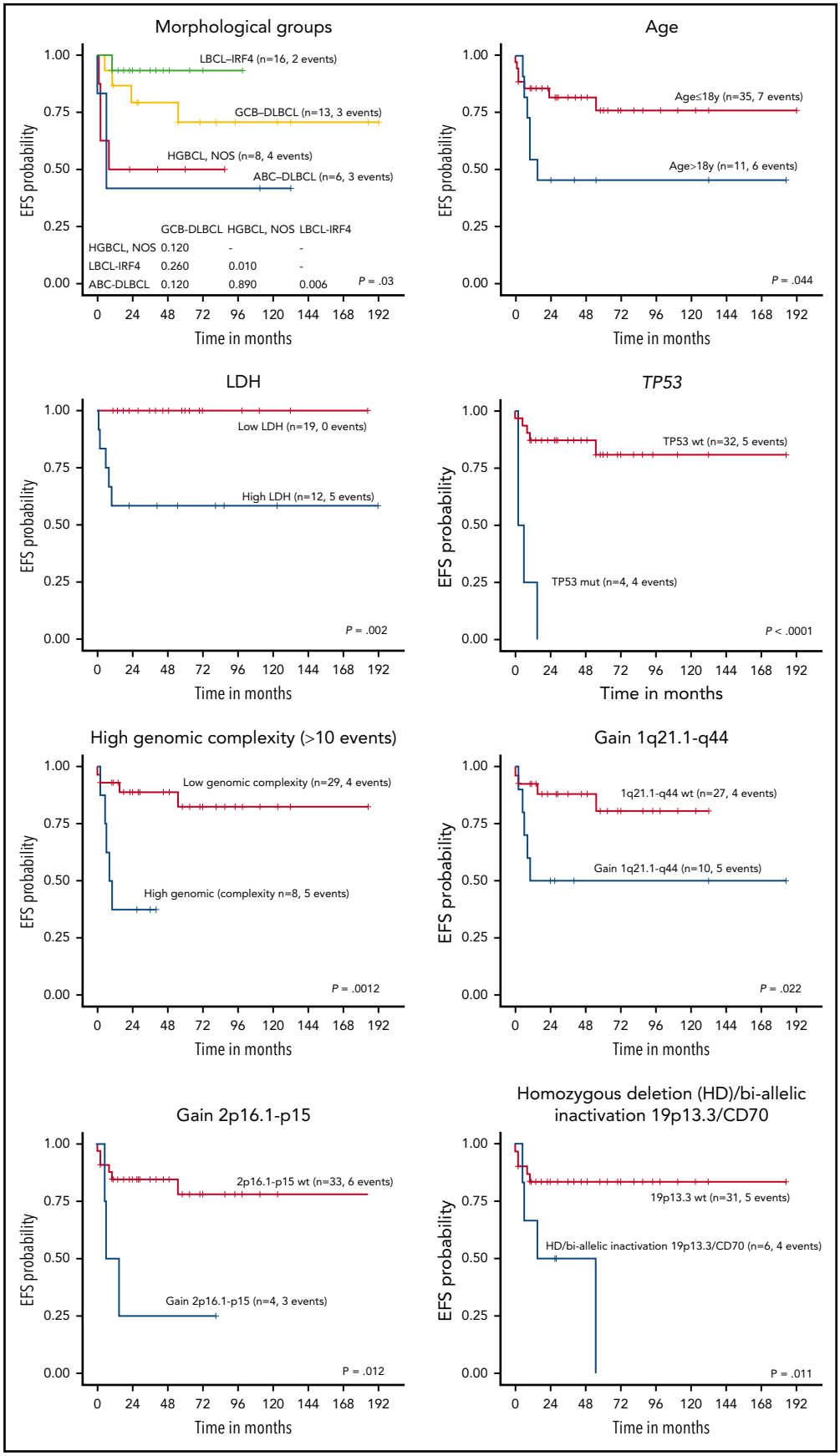

Figure 6. EFS of 45 pediatric and young adult LBCL cases according to morphological and molecular subtypes, age, LDH levels, and specific molecular features. wt, wild type.

affecting the *IRF4* gene with an aSHM pattern appears to be a hallmark of the *IRF4* translocation. Further studies are needed to define the potential functional effect of these mutations. Morphologically, LBCL-*IRF4* may have predominantly diffuse or follicular pattern. Interestingly, *CARD11* mutations were seen exclusively in cases with diffuse growth pattern, whereas *MAP2K1* mutations, characteristic of pediatric-type follicular lymphoma,[37,38] were detected in 2 cases with a predominantly follicular pattern (supplemental Figure 8), suggesting that the underlying mutational profile may influence the morphological features of the tumors. No differences in terms of CN mutational profile, including *IRF4* mutations and IRF4 expression at the RNA and protein level (supplemental Figure 3), were seen in the 2 LBCL-*IRF4* cases with an IGH split without concomitant *IRF4* breaks, confirming the idea that these tumors belong to the same entity. The presence of cryptic *IRF4* translocations cannot be excluded.[45] The outcome of LBCL-*IRF4* was very favorable, but most of the patients were treated with aggressive pediatric or adult-type chemotherapy protocols. The identification of the translocation and the related mutational profile may be relevant to identify these patients and design management strategies better suited to the biology of the tumors.[17,19]

The genetic and expression profile of our DLBCL, NOS was relatively similar to that previously observed in pediatric cohorts with a predominance of GCB-DLBCL, low CN complexity, few *MYC* and *BCL6* rearrangements, and, in contrast to adults, the virtual absence of *BCL2* translocations (supplemental Table 15).[46-48] Our study expands these observations, showing that these cases have a mutational profile similar to adult DLBCL with predominance of mutations in GCB-DLBCL–related genes (supplemental Figures 5 and 8). Nevertheless, pediatric and young adult DLBCL had higher frequency of *SOCS1* mutations and virtually lacked *MYD88*-L265P, *NOTCH1*, *NOTCH2*, *BCL2*, and *SGK1* mutations that have been associated with the definition of established mutational clusters in adult DLBCL.[5,6] Further studies using whole-exome/genome approaches may expand the genomic profile of alterations of these tumors.

The application of the Lymph3Cx in our DLBCL, NOS cohort recognized 4 cases predicted as mPMBL with an atypical clinical presentation for this entity.[32] Although 3 of these patients had mediastinal lymph node involvement, they also had disseminated disease including bone marrow and extranodal involvement. Intriguingly, 1 case predicted as mPMBL only had axillary nodal involvement. The mutational profile of these cases was consistent with PMBL, including *NFKBIE* mutations recently associated with poor outcome in these tumors.[49] These observations, together with similar cases recently described in adults, suggest that a subset of DLBCL, NOS in pediatric and young adult populations may correspond to PMBL.[34,50]

The genetic features of HGBCL, NOS were heterogeneous. Four out of the 8 molecularly investigated cases had mutational profile closer to BL (supplemental Figure 5), with concomitant *MYC* rearrangements and 1q21-q31 gains identified in 2 cases each (Figure 3E; supplemental Figure 4). Nevertheless, those cases did not have the typical BL morphology and expressed strong BCL2 or MUM1. Similar to HGBCL, NOS in adults,[22,23] no *TCF3* mutations were seen in our cases. Other HGBCL, NOS cases had mutational profiles closer to GCB-DLBCL with *TNFRSF14*, *CARD11*, and *EZH2* mutations and lacked *MYC* translocations. Of note, genes frequently mutated in BLL-11q, such as *BTG2*, *ETS1*, and *EP300*,[15,16] were significantly absent in both DLBCL and HGBCL, NOS ($P < .05$), suggesting that they correspond to different entities (supplemental Figure 5).

Regarding prognostic aspects, advanced stage, high LDH, and combined bone marrow and central nervous system disease have been significantly associated with unfavorable outcome in pediatric mature B-cell lymphomas, whereas the adverse prognosis of 8q24-*MYC* rearrangements and ABC-COO is still controversial.[24,27] In our series, we found the prognostic value of several clinical and molecular features such as age >18 years, high LDH levels, and ABC-subtype, as seen in adult populations. We also found that *TP53* mutations, high genetic complexity, including chromothripsis, and gains in 1q21-q44/*MDM4* conferred poor EFS.

In conclusion, LBCLs in the pediatric and young adult population are a heterogeneous group of tumors with distinct genomic and mutational alterations. LBCL-*IRF4* reveals a GC phenotype with frequent mutations in *IRF4*, NF-κB-related genes (*CARD11*, *CD79B*, and *MYD88*), and overexpression of genes of the NF-κB pathway, whereas DLBCL, NOS cases in this population are predominantly of GCB subtype. Our study also suggests that PMBL may present with disseminated disease, and ancillary tools may recognize these cases, with implications for treatment. The integration of molecular and genetic studies may improve the classification of LBCL in pediatric and young adult populations and provide parameters for risk stratification.

Acknowledgments

The authors thank the centers of the Sociedad Española de Hematología y Oncología Pediátricas that submitted cases for consultation, as well as Noelia Garcia, Silvia Martín, and Helena Suarez for their excellent technical assistance. They also thank Miguel Angel Piris from Fundación Jimenez Díaz for performing immunohistochemical analyses and Pedro Jares and Magda Pinyol from Hospital Clínic, Institut d'Investigacions Biomèdiques August Pi i Sunyer (IDIBAPS) for their support with gene expression analyses. The authors are indebted to the IDIBAPS Genomics Core Facility and the HCB-IDIBAPS Biobank-Tumor Bank and Biobanc de l'Hospital Infantil Sant Joan de Déu, Hospital Universitario Virgen del Rocío-Instituto de Biomedicina de Sevilla Biobank (ISCIII-Red de Biobancos PT13/0010/0056), all 3 integrated in the National Network Biobanks of ISCIII, for the sample and data procurement.

This work was supported by Asociación Española Contra el Cáncer (AECC CICPFI6025SALA), Fondo de Investigaciones Sanitarias Instituto de Salud Carlos III (Miguel Servet Program CP13/00159 and PI15/00580 to I.S.), Spanish Ministerio de Economía y Competitividad (SAF2015-64885-R to E.C.), Generalitat de Catalunya Suport Grups de Recerca (2017-SGR-1107 to I.S. and 2017-SGR-1142 to E.C.), SPECS II grant (National Cancer Institute 1U01CA157581), and the European Regional Development Fund (Una manera de fer Europa). J.E.R.-Z. was supported by a fellowship from Generalitat de Catalunya AGAUR FI-DGR 2017 (2017 FI_B01004). E.C. is an Academia Researcher of the Institució Catalana de Recerca i Estudis Avançats of the Generalitat de Catalunya. This work was developed at the Centro Esther Koplowitz, Barcelona, Spain. The group is supported by Acció instrumental d'incorporació de científics i tecnòlegs PERIS 2016 (SLT002/16/00336 to Noelia Garcia) from Generalitat de Catalunya.

Authorship

Contribution: J.E.R.-Z. performed research, analyzed data, and wrote the manuscript; B.G.-F. performed morphological diagnosis, analyzed data, and wrote the paper; F.N., J.S.-V., I.M.-G., G.C., A.E., A. Maguire, and

C.R. performed research and analyzed data; O.B., M.G.-P., A.G., M.S., D.A., C.B., F.G.-B., G.T., A. Mozos, L.M.R., L.Q.-M., and E.S.J. reviewed and interpreted pathological data; V.C., M. Andrés, M. Andión, I.A., M.S.d.I., C.S., S.G., J.V.-A., R.F.-D., A.R.-D., V.P., M.T., P.S.-P., I.D., A.L.-G., P.G., and M.J.O. reviewed and interpreted clinical data; E.C. performed morphological analysis, designed research, and wrote the manuscript; and I.S. performed research, analyzed data, designed research, and wrote the manuscript; and all authors approved the final manuscript.

Conflict-of-interest disclosure: E.C. and L.M.R. are co-inventors of the Lymph2Cx and Lymph3Cx gene expression profiling assay used in this study. The remaining authors declare no competing financial interests.

ORCID profiles: J.E.R.-Z., 0000-0001-7108-7738; B.G.-F., 0000-0002-1796-7248; O.B., 0000-0002-5099-3675; F.N., 0000-0003-2910-9440; I.M.-G., 0000-0002-0098-1908; M.G.-P., 0000-0002-7762-7085; A.G., 0000-0003-0324-2251; M.S.d.I., 0000-0002-8054-9698; C.S., 0000-0003-3956-5466; S.G., 0000-0002-4712-9624; V.P., 0000-0002-2668-3263; A. Mozos, 0000-0002-3350-1827; M.J.O., 0000-0001-6419-2513; A. Maguire, 0000-0002-1193-5528; L.Q.-M., 0000-0001-7156-5365; E.S.J., 0000-0003-4632-0301; E.C., 0000-0001-9850-9793; I.S., 0000-0002-2427-9822.

Correspondence: Itziar Salaverria, Institut d'Investigacions Biomèdiques August Pi i Sunyer (IDIBAPS), Rosselló 149-153, 08036 Barcelona, Spain; e-mail: isalaver@clinic.cat.

Footnotes

Submitted 8 August 2019; accepted 31 October 2019; prepublished online on *Blood* First Edition 18 November 2019. DOI 10.1182/blood.2019002699.

*J.E.R.-Z. and B.G.-F. contributed equally to this study.

The CN and gene expression data reported in this article have been deposited to the GEO database under accession number GSE128294. Sequencing data have been deposited to the European Nucleotide Archive under accession number ERP114095.

The online version of this article contains a data supplement.

The publication costs of this article were defrayed in part by page charge payment. Therefore, and solely to indicate this fact, this article is hereby marked "advertisement" in accordance with 18 USC section 1734.

REFERENCES

1. Dunleavy K, Gross TG. Management of aggressive B-cell NHLs in the AYA population: an adult vs pediatric perspective. *Blood*. 2018; 132(4):369-375.
2. Pasqualucci L, Trifonov V, Fabbri G, et al. Analysis of the coding genome of diffuse large B-cell lymphoma. *Nat Genet*. 2011;43(9): 830-837.
3. Morin RD, Mungall K, Pleasance E, et al. Mutational and structural analysis of diffuse large B-cell lymphoma using whole-genome sequencing. *Blood*. 2013;122(7):1256-1265.
4. Lohr JG, Stojanov P, Lawrence MS, et al. Discovery and prioritization of somatic mutations in diffuse large B-cell lymphoma (DLBCL) by whole-exome sequencing. *Proc Natl Acad Sci USA*. 2012;109(10):3879-3884.
5. Chapuy B, Stewart C, Dunford AJ, et al. Molecular subtypes of diffuse large B cell lymphoma are associated with distinct pathogenic mechanisms and outcomes [published correction appears in *Nat Med*. 2018;24(8): 1290-1291]. *Nat Med*. 2018;24(5):679-690.
6. Schmitz R, Wright GW, Huang DW, et al. Genetics and pathogenesis of diffuse large B-cell lymphoma. *N Engl J Med*. 2018;378(15): 1396-1407.
7. Reddy A, Zhang J, Davis NS, et al. Genetic and functional drivers of diffuse large B cell lymphoma. *Cell*. 2017;171(2):481-494.e15.
8. Savage KJ, Monti S, Kutok JL, et al. The molecular signature of mediastinal large B-cell lymphoma differs from that of other diffuse large B-cell lymphomas and shares features with classical Hodgkin lymphoma. *Blood*. 2003;102(12):3871-3879.
9. Richter J, Schlesner M, Hoffmann S, et al; ICGC MMML-Seq Project. Recurrent mutation of the ID3 gene in Burkitt lymphoma identified by integrated genome, exome and transcriptome sequencing. *Nat Genet*. 2012; 44(12):1316-1320.
10. Love C, Sun Z, Jima D, et al. The genetic landscape of mutations in Burkitt lymphoma. *Nat Genet*. 2012;44(12):1321-1325.
11. Schmitz R, Young RM, Ceribelli M, et al. Burkitt lymphoma pathogenesis and therapeutic targets from structural and functional genomics. *Nature*. 2012;490(7418):116-120.
12. Dunleavy K. Primary mediastinal B-cell lymphoma: biology and evolving therapeutic strategies. *Hematology Am Soc Hematol Educ Program*. 2017;2017:298-303.
13. In: Swerdlow SH, Campo E, Harris NL, eds., et al. WHO Classification of Tumours of Haematopoietic and Lymphoid Tissues, Revised 4th ed, Lyon: IARC; 2017:
14. Salaverria I, Martin-Guerrero I, Wagener R, et al; Berlin-Frankfurt-Münster Non-Hodgkin Lymphoma Group. A recurrent 11q aberration pattern characterizes a subset of MYC-negative high-grade B-cell lymphomas resembling Burkitt lymphoma. *Blood*. 2014; 123(8):1187-1198.
15. Gonzalez-Farre B, Ramis-Zaldivar JE, Salmeron-Villalobos J, et al. Burkitt-like lymphoma with 11q aberration: a germinal center-derived lymphoma genetically unrelated to Burkitt lymphoma. *Haematologica*. 2019; 104(9):1822-1829.
16. Wagener R, Seufert J, Raimondi F, et al. The mutational landscape of Burkitt-like lymphoma with 11q aberration is distinct from that of Burkitt lymphoma. *Blood*. 2019;133(9): 962-966.
17. Salaverria I, Philipp C, Oschlies I, et al; Berlin-Frankfurt-Münster-NHL trial group. Translocations activating IRF4 identify a subtype of germinal center-derived B-cell lymphoma affecting predominantly children and young adults. *Blood*. 2011;118(1):139-147.
18. Quintanilla-Martinez L, Sander B, Chan JK, et al. Indolent lymphomas in the pediatric population: follicular lymphoma, IRF4/MUM1+ lymphoma, nodal marginal zone lymphoma and chronic lymphocytic leukemia. *Virchows Arch*. 2016;468(2):141-157.
19. Chisholm KM, Mohlman J, Liew M, et al. IRF4 translocation status in pediatric follicular and diffuse large B-cell lymphoma patients enrolled in Children's Oncology Group trials. *Pediatr Blood Cancer*. 2019;66(8):e27770.
20. Woessmann W, Quintanilla-Martinez L. Rare mature B-cell lymphomas in children and adolescents. *Hematol Oncol*. 2019;37(suppl 1):53-61.
21. Salaverria I, Martin-Guerrero I, Burkhardt B, et al. High resolution copy number analysis of IRF4 translocation-positive diffuse large B-cell and follicular lymphomas. *Genes Chromosomes Cancer*. 2013;52(2):150-155.
22. Momose S, Weißbach S, Pischimarov J, et al. The diagnostic gray zone between Burkitt lymphoma and diffuse large B-cell lymphoma is also a gray zone of the mutational spectrum. *Leukemia*. 2015;29(8):1789-1791.
23. Sha C, Barrans S, Cucco F, et al. Molecular high-grade B-cell lymphoma: defining a poor-risk group that requires different approaches to therapy. *J Clin Oncol*. 2019;37(3):202-212.
24. Poirel HA, Cairo MS, Heerema NA, et al; FAB/LMB 96 International Study Committee. Specific cytogenetic abnormalities are associated with a significantly inferior outcome in children and adolescents with mature B-cell non-Hodgkin's lymphoma: results of the FAB/LMB 96 international study. *Leukemia*. 2009; 23(2):323-331.
25. Rosenwald A, Wright G, Chan WC, et al; Lymphoma/Leukemia Molecular Profiling Project. The use of molecular profiling to predict survival after chemotherapy for diffuse large-B-cell lymphoma. *N Engl J Med*. 2002; 346(25):1937-1947.
26. Karube K, Enjuanes A, Dlouhy I, et al. Integrating genomic alterations in diffuse large B-cell lymphoma identifies new relevant pathways and potential therapeutic targets. *Leukemia*. 2018;32(3):675-684.
27. Szczepanowski M, Lange J, Kohler CW, et al. Cell-of-origin classification by gene expression and MYC-rearrangements in diffuse large B-cell lymphoma of children and adolescents. *Br J Haematol*. 2017;179(1):116-119.
28. Hans CP, Weisenburger DD, Greiner TC, et al. Confirmation of the molecular classification of diffuse large B-cell lymphoma by immunohistochemistry using a tissue microarray. *Blood*. 2004;103(1):275-282.

29. Steidl C, Shah SP, Woolcock BW, et al. MHC class II transactivator CIITA is a recurrent gene fusion partner in lymphoid cancers. *Nature*. 2011;471(7338):377-381.

30. Scholtysik R, Kreuz M, Klapper W, et al; Molecular Mechanisms in Malignant Lymphomas Network Project of Deutsche Krebshilfe. Detection of genomic aberrations in molecularly defined Burkitt's lymphoma by array-based, high resolution, single nucleotide polymorphism analysis. *Haematologica*. 2010; 95(12):2047-2055.

31. Scott DW, Wright GW, Williams PM, et al. Determining cell-of-origin subtypes of diffuse large B-cell lymphoma using gene expression in formalin-fixed paraffin-embedded tissue. *Blood*. 2014;123(8):1214-1217.

32. Mottok A, Wright G, Rosenwald A, et al. Molecular classification of primary mediastinal large B-cell lymphoma using routinely available tissue specimens. *Blood*. 2018;132(22): 2401-2405.

33. Cheson BD, Pfistner B, Juweid ME, et al; International Harmonization Project on Lymphoma. Revised response criteria for malignant lymphoma. *J Clin Oncol*. 2007; 25(5):579-586.

34. Yuan J, Wright G, Rosenwald A, et al; Lymphoma Leukemia Molecular Profiling Project (LLMPP). Identification of primary mediastinal large B-cell lymphoma at nonmediastinal sites by gene expression profiling. *Am J Surg Pathol*. 2015;39(10):1322-1330.

35. Lenz G, Davis RE, Ngo VN, et al. Oncogenic CARD11 mutations in human diffuse large B cell lymphoma. *Science*. 2008;319(5870): 1676-1679.

36. Davis RE, Ngo VN, Lenz G, et al. Chronic active B-cell-receptor signalling in diffuse large B-cell lymphoma. *Nature*. 2010; 463(7277):88-92.

37. Louissaint A Jr., Schafernak KT, Geyer JT, et al. Pediatric-type nodal follicular lymphoma: a biologically distinct lymphoma with frequent MAPK pathway mutations. *Blood*. 2016; 128(8):1093-1100.

38. Schmidt J, Ramis-Zaldivar JE, Nadeu F, et al. Mutations of *MAP2K1* are frequent in pediatric-type follicular lymphoma and result in ERK pathway activation. *Blood*. 2017; 130(3):323-327.

39. Saito M, Gao J, Basso K, et al. A signaling pathway mediating downregulation of BCL6 in germinal center B cells is blocked by BCL6 gene alterations in B cell lymphoma. *Cancer Cell*. 2007;12(3):280-292.

40. López C, Kleinheinz K, Aukema SM, et al; ICGC MMML-Seq Consortium. Genomic and transcriptomic changes complement each other in the pathogenesis of sporadic Burkitt lymphoma. *Nat Commun*. 2019;10(1):1459.

41. Khodabakhshi AH, Morin RD, Fejes AP, et al. Recurrent targets of aberrant somatic hypermutation in lymphoma. *Oncotarget*. 2012; 3(11):1308-1319.

42. Wagener R, Bens S, Toprak UH, et al. Cryptic insertion of *MYC* exons 2 and 3 into the IGH locus detected by whole genome sequencing in a case of MYC-negative Burkitt lymphoma [published online ahead of print 9 May 2019]. *Haematologica*. doi:10.3324/haematol.2018.208140.

43. Edelmann J, Holzmann K, Miller F, et al. High-resolution genomic profiling of chronic lymphocytic leukemia reveals new recurrent genomic alterations. *Blood*. 2012;120(24): 4783-4794.

44. Yang Y, Shaffer AL III, Emre NC, et al. Exploiting synthetic lethality for the therapy of ABC diffuse large B cell lymphoma. *Cancer Cell*. 2012;21(6):723-737.

45. Liu Q, Salaverria I, Pittaluga S, et al. Follicular lymphomas in children and young adults: a comparison of the pediatric variant with usual follicular lymphoma. *Am J Surg Pathol*. 2013; 37(3):333-343.

46. Oschlies I, Klapper W, Zimmermann M, et al. Diffuse large B-cell lymphoma in pediatric patients belongs predominantly to the germinal-center type B-cell lymphomas: a clinicopathologic analysis of cases included in the German BFM (Berlin-Frankfurt-Munster) Multicenter Trial. *Blood*. 2006;107(10): 4047-4052.

47. Klapper W, Kreuz M, Kohler CW, et al; Molecular Mechanisms in Malignant Lymphomas Network Project of the Deutsche Krebshilfe. Patient age at diagnosis is associated with the molecular characteristics of diffuse large B-cell lymphoma. *Blood*. 2012;119(8):1882-1887.

48. Deffenbacher KE, Iqbal J, Sanger W, et al. Molecular distinctions between pediatric and adult mature B-cell non-Hodgkin lymphomas identified through genomic profiling. *Blood*. 2012;119(16):3757-3766.

49. Mansouri L, Noerenberg D, Young E, et al. Frequent NFKBIE deletions are associated with poor outcome in primary mediastinal B-cell lymphoma. *Blood*. 2016;128(23): 2666-2670.

50. Chen BJ, Ruminy P, Roth CG, et al. Cyclin D1-positive mediastinal large B-cell lymphoma with copy number gains of CCND1 gene: a study of 3 cases with nonmediastinal disease. *Am J Surg Pathol*. 2019;43(1):110-120.